Journal of Structural Biology xxx (xxxx) xxx–xxx

Contents lists available at ScienceDirect

Journal of Structural Biology

journal homepage: www.elsevier.com/locate/yjsbi

Structures of kobuviral and siciniviral polymerases reveal conserved mechanism of picornaviral polymerase activation

Anna Dubankova, Vladimira Horova, Martin Klima, Evzen Boura*

Institute of Organic Chemistry and Biochemistry of the Czech Academy of Sciences, Flemingovo nam. 2., 166 10 Prague 6, Czech Republic

ARTICLE INFO

Keywords:
RNA
Polymerase
Crystal structure
Kobuvirus
Picornavirus

ABSTRACT

RNA-dependent RNA polymerase $3D^{pol}$ is a key enzyme for the replication of picornaviruses. The viral genome is translated into a single polyprotein that is subsequently proteolytically processed into matured products. The $3D^{pol}$ enzyme arises from a stable 3CD precursor that has high proteolytic activity but no polymerase activity. Upon cleavage of the precursor the newly established N-terminus of $3D^{pol}$ is liberated and inserts itself into a pocket on the surface of the $3D^{pol}$ enzyme. The essential residue for this mechanism is the very first glycine that is conserved among almost all picornaviruses. However, kobuviruses and siciniviruses have a serine residue instead. Intrigued by this anomaly we sought to solve the crystal structure of these $3D^{pol}$ enzymes. The structures revealed a unique fold of the $3D^{pol}$ N-termini but the very first serine residues were inserted into a charged pocket in a similar manner as the glycine residue in other picornaviruses. These structures revealed a common underlying mechanism of $3D^{pol}$ activation that lies in activation of the α10 helix containing a key catalytical residue Asp238 that forms a hydrogen bond with the 2′ hydroxyl group of the incoming NTP nucleotide.

1. Introduction

Positive-sense single stranded RNA viruses (+RNA viruses) are a large group of viruses (e.g. Picornavirales, Nidovirales, Tymovirales) that are comprised of many families. The *Picornaviridae* family includes many dangerous human pathogens such as poliovirus (PV), coxsackievirus, hepatitis A virus and some ostensibly less dangerous pathogens such as rhinoviruses (common cold) and kobuviruses (gastroenteritis). The picornaviral genome also serves as mRNA and is translated into a single polyprotein that is later processed into structural (VP0–VP4) and non-structural (2A, 2B, 2C, 3A, 3B, 3C, 3D) proteins, a leader (L) protein is also present in some picornaviruses (Fig. 1A) that together with many host factors ensure viral replication. The replication takes place at membranous replication organelles (ROs) that serve as a rendezvous place for viral proteins and perhaps also as a shelter from innate immunity (Harak and Lohmann, 2015; Nagy et al., 2016). ROs are usually multilamellar and enriched in specific lipids such as phosphatidylinositol 4-phosphate (PI4P) and cholesterol (Altan-Bonnet, 2017). It was suggested that PI4P directly recruits the viral polymerase to the ROs (Hsu et al., 2010) although recent results suggest that a negative charge in general rather than PI4P specifically is responsible for $3D^{pol}$ recruitment to the membrane (Dubankova et al., 2017).

A key enzyme for replication of RNA viruses is the RNA-dependent RNA polymerase (RdRp – termed $3D^{pol}$ in picornaviruses) because such an enzyme is not present in the eukaryotic cell and each RNA virus must encode for it. The mature $3D^{pol}$ enzyme arises from the cleavage of the stable 3CD precursor that itself arises from the single polyprotein. Interestingly, 3CD has no polymerase activity but does have high proteolytical activity (Harris et al., 1992; Sun et al., 2016). The prototypical $3D^{pol}$ enzyme is the PV polymerase that is best biochemically characterized (for a thorough recent review, see (Peersen, 2017)). $3D^{pol}$ has many unique features. Most importantly, it has low fidelity, which is responsible for the origin and distribution of quasispecies (mutant clouds established in infected organisms) (Andino and Domingo, 2015). Interestingly, it uses a protein primer – a short peptide (~22 AAs) called 3B or VPg (from viral protein genome linked) – that has a conserved tyrosine residue at position 3 and its hydroxyl group serves as the attachment point for the first nucleotide (Paul et al., 1998). Deep molecular insight into the structure of picornaviral $3D^{pol}$ enzymes was gained over the last decades as many were crystallized including the PV, coxsackie, FMDV, rhinovirus and enterovirus 71 polymerase (Campagnola et al., 2008; Ferrer-Orta et al., 2004; Hansen et al., 1997; Love et al., 2004; Thompson and Peersen, 2004; Wu et al., 2010) which were also crystallized in complex with RNA (Ferrer-Orta et al., 2004; Ferrer-Orta et al., 2007; Gong and Peersen, 2010; Gong et al., 2013). All the structures show the conserved right-hand fold typical for viral RNA

* Corresponding author.
E-mail address: boura@uochb.cas.cz (E. Boura).

https://doi.org/10.1016/j.jsb.2019.08.004
Received 28 June 2019; Received in revised form 8 August 2019; Accepted 9 August 2019

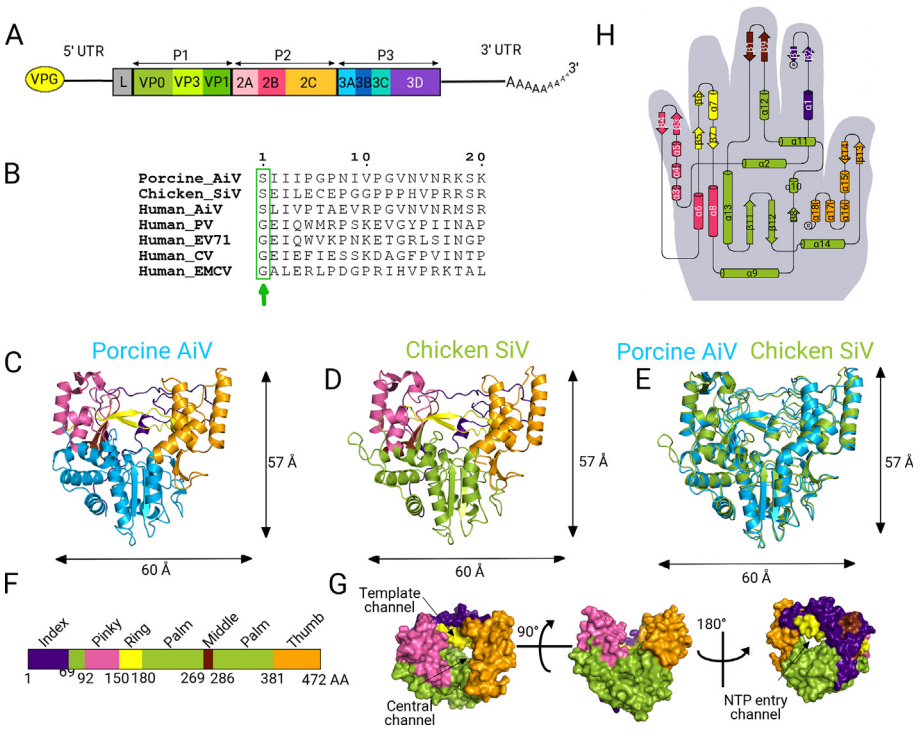

Fig. 1. Overall fold of Aichi 3D^{pol} enzyme. A) Aichi RNA genome organization: P1 region encodes structural proteins VP0, VP3 and VP1. While the P2 and P3 regions encode for non-structural proteins. The sequence encoding 3D^{pol} gene is located on the very 3′ end. B) Multiple alignment illustrates that kobuviruses (AiV) have conserved serine residue at the very N-termini of 3D^{pol} where all other picornaviruses have a glycine residue C and D) Structure of the porcine AiV 3D^{pol} with palm, thumb and fingers (index, middle, ring, pinky) domains. E) Superposition of the AiV and SiV 3D^{pol} enzymes reveals virtually identical fold. G) The location of the template, central and NTP entry channel within the 3D^{pol} AiV structure. H) The 3D^{pol} topology plot drawn on a silhouette of a right hand.

polymerases with the central RNA template channel. Interestingly, all the above mentioned RNA polymerases share the very first conserved glycine residues. Comparison of the crystal structure of the precursor protein 3CD with the mature 3D^{pol} protein (Marcotte et al., 2007) reveals that upon cleavage the N-terminus undergoes a conformational change which is essential for 3D^{pol} activation. For instance, a single amino acid residue in excess renders the 3D^{pol} enzyme inactive, which is important to take into account when producing the protein recombinantly (Gohara et al., 1999). Only seven genera (Kobuviruses, Galliviruses, Osciviruses, Passeriviruse, Sakobuviruses, Saliviruses and Siciniviruses) of the *Picornaviridae* family do not possess this conserved glycine residue and have a serine residue instead (SI Fig. 1).

Kobuviruses infect many mammalian species. The human kobuvirus was first isolated in the Japanese prefecture Aichi from a patient with acute gastroenteritis and was afterwards termed human Aichi virus (Yamashita et al., 1991). Aichi virus is a very common pathogen (more than 80% of adults have antibodies against it) and globally distributed (Kitajima and Gerba, 2015). Recently, Aichi virus also attracted scientific attention. It was crystallized revealing the mechanism of kobuvirus genome release (Sabin et al., 2016) and its replication was described as PI4KB (phosphatidylinositol 4-kinase B, one of four human enzymes that synthesize PI4P) dependent (Greninger et al., 2012; Sasaki et al., 2012). Congruently, inhibitors of PI4KB inhibit Aichi virus replication (Mejdrova et al., 2015; Mejdrova et al., 2017). Recently we solved the crystal structure of the Aichi 3A protein in complex with the GOLD domain of ACBD3 (Acyl-CoA-binding domain-containing protein 3, a Golgi resident protein and a nanomolar binder of PI4KB). The structure revealed that the 3A protein that is intrinsically disordered by itself, however, in the complex adopts a highly ordered structure and literally wraps around the GOLD domain of ACBD3 to hijack PI4KB to bring it to target membrane and activate it (Klima et al., 2017; Klima et al., 2016), a mechanism that is shared with enteroviruses (Horova et al., 2019). Confirming results were also reached using mass spectroscopy (McPhail et al., 2017). Still many features of kobuviruses including mechanism of replication remain unexplained. Sicinivirus is a new picornavirus genus that remains to be described in detail (Bullman et al., 2014). Here, we describe the atomic structures of the key enzyme – the RNA-dependent RNA polymerase 3D^{pol} of the Aichi virus (kobuvirus) and the Sicinivirus A.

2. Results

We sought to solve the crystal structure of the 3D^{pol} enzymes that have unique sequences at their N-termini – a serine residue where all other picornaviruses have a glycine residue (Fig. 1B, SI Fig. 1). We have screened several 3D^{pol} enzymes for the ability to form well diffracting crystals (Table 1) and discovered that the 3D^{pol} from the porcine Aichi virus and chicken Sicinivirus A form well diffracting crystals after the introduction of crystal-stabilizing mutations (detailed in M&M section).

The structures were solved by molecular replacement and revealed the classical right-hand fold consisting of fingers palm and thumb, with fingers subdivided in index, middle, ring and pinky (Fig. 1). The enzyme is comprised of 18 helices and 14 beta strands that make up the

Table 1
Statistics of crystallographic data collection and refinement.

Data collection		
Crystal	Sicinivirus 3D^{pol}	Aichi virus 3D^{pol}
Space group	$P4_22_12$	$P6_122$
Cell dimension	a = b = 92.5 Å, c = 161.0 Å	a = b = 170.5 Å, 231.3 Å
X-ray source	BESSY ID 14-1	BESSY ID 14-1
Resolution (Å)	46.62–2.30 (2.38–2.30)	48.13–2.64 (2.73–2.64)
Unique reflections	31,996 (3120)	59,076 (5790)
I/σ (I)	13.40 (2.10)	33.96 (4.98)
Wavelength (Å)	0.9184	0.9184
Multiplicity	14.0 (9.8)	21.9 (22.2)
Completeness (%)	99.93 (99.58)	99.96 (100.00)
R-merge, %	19.1 (100)	8.5 (67.8)
$CC_{1/2}$	0.997 (0.791)	1 (0.94)
Refinement		
R-work, %	19.18 (25.95)	19.10 (24.16)
R-free, %	22.46 (31.45)	22.19 (26.43)
RMS (bonds), °	0.009	0.004
RMS (angles), Å	1.11	0.76
Ramachandran (outliers/favored) (%)	0.85%/97.66%	0%/98.28%

Numbers in parentheses refer to the highest resolution shell.

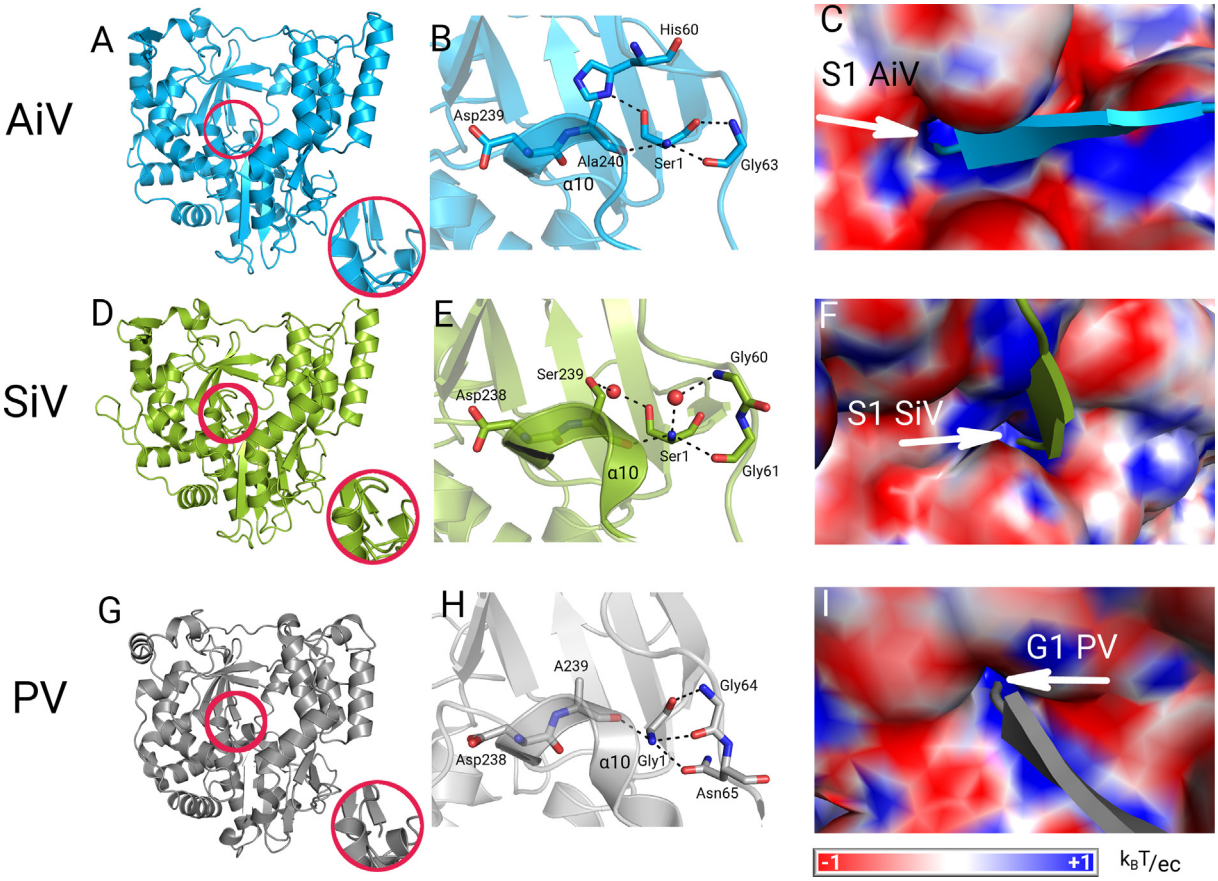

Fig. 2. Atypical fold of N termini of AiV and SiV 3D^{pol} among 3D^{pol} enzymes. A-C) The first residue of AiV 3D^{pol} is locked to a positively charged cavity leading to protein center by residues H40, G63 and A240. D-F) Corresponding view of the SiV 3D^{pol} structure. G-I) All other picornaviruses have the first glycine residue inserted in a charged cavity as illustrated by the PV 3D^{pol} structure.

six subdomains that we recognize within the polymerase family: thumb, index (α15-18, β13-14), middle (β9-10), ring (α7, β5-7), and pinky (α3-6, α8, β3-4) fingers and the palm (α2, α9-13, β8, β11-12) (Fig. 1H). We could also identify the three characteristic channels, the template binding, central and NTP entry channel (Fig. 1D) (Ferrer-Orta et al., 2006; Peersen, 2017). The template channel is surrounded by the palm domain and the ring and pinky fingers. It is further stabilized by the middle finger and wrapped around by the index finger. The central channel is located next to the template channel and is surrounded mainly by the palm domain and the ring finger. The third channel is the NTP entry channel. The structure of the NTP entry channel is created by the interaction of the ring finger and the palm domain. The index and thumb fingers are wrapped around the NTP channel and stabilize it (Fig. 1).

As mentioned, the first N-terminal residue (a glycine in all previously solved structures) of picornaviral polymerases inserts itself into a pocked within the enzyme (Fig. 2). The first residue is absolutely essential for the 3D^{pol} activity and is also well visible in our structures (SI Fig. 2) and its deletion or mutation leads to an inactive enzyme as was shown for the Coxsackie virus 3D^{pol} (Campagnola et al., 2008). In case of PV the first glycine residue forms a hydrogen bond with N65 (Thompson and Peersen, 2004). The first AiV serine residue forms hydrogen bonds with H60, G63 and A240 while the first SiV 3D^{pol} serine residue forms a water bridge with S239 (Fig. 2, for superposition with other picornaviral polymerases, please, see SI Fig. 3). We aimed to test the importance of the first serine residue using mutational analysis. Unfortunately, the AiV and SiV 3D^{pol} enzymes have only negligible activity *in vitro* under the same conditions where the PV polymerase is active (SI Fig. 4). Therefore, we devised a subgenomic replicon assay in cells. First, we replaced the P1 genomic fragment encoding the viral structural proteins by a sequence encoding the fluorescent protein mCherry generating the pUCSF-AiV/mCherry plasmid. Next, we introduced several mutations (Ser1Gly, Ser1Ala, +1Ser, +1Gly, +2Ser, and Δ3D^{pol}) and we tested the replication of the appropriate RNA in cell culture using FACS analysis (fluorescence-activated cell sorter, detailed in M&M) (Fig. 3). We observed efficient replication of the wild type RNA. The intensity of fluorescence in the case of the 3D^{pol} deletion mutant (Δ3D^{pol}) was two orders of magnitude lower and we consider this value as zero because the Δ3D^{pol} RNA cannot replicate and the whole signal comes from the translation of the original transfected RNA only. No replication was also observed for all the mutants with additional N-terminal residues (+1x Ser, +1x Gly, +2x Ser) and only very inefficient replication (~5% of wt) for Ser1Gly and Ser1Ala mutants. Ser1Ala mutant RNA also replicated inefficiently (~10% of wt). However, the 3CD precursor processing test revealed that the mutants + 1Ser and + 2Ser are rapidly degraded in cells (Fig. 3D) at the same conditions where the wild type 3CD is properly processed as expected and so are the mutants Ser1Gly, Ser1Ala, and + 1Gly. The mutations + 1Ser and + 2Ser are deleterious for the enzyme in cells and thus enzymatic activity of these mutants could not be tested.

These results demonstrate that a proper processing of the 3D^{pol} N-terminus is absolutely essential in the case of 3D^{pol} enzymes possessing a serine residue in the first position just as for the typical glycine-starting polymerases. Even mutation of the first serine residue to glycine mimicking all other picornaviruses is not tolerated.

3. Discussion

The main motivation of this study was to decipher the role of the very first 3D^{pol} serine residue that is present in the kobuvirus and

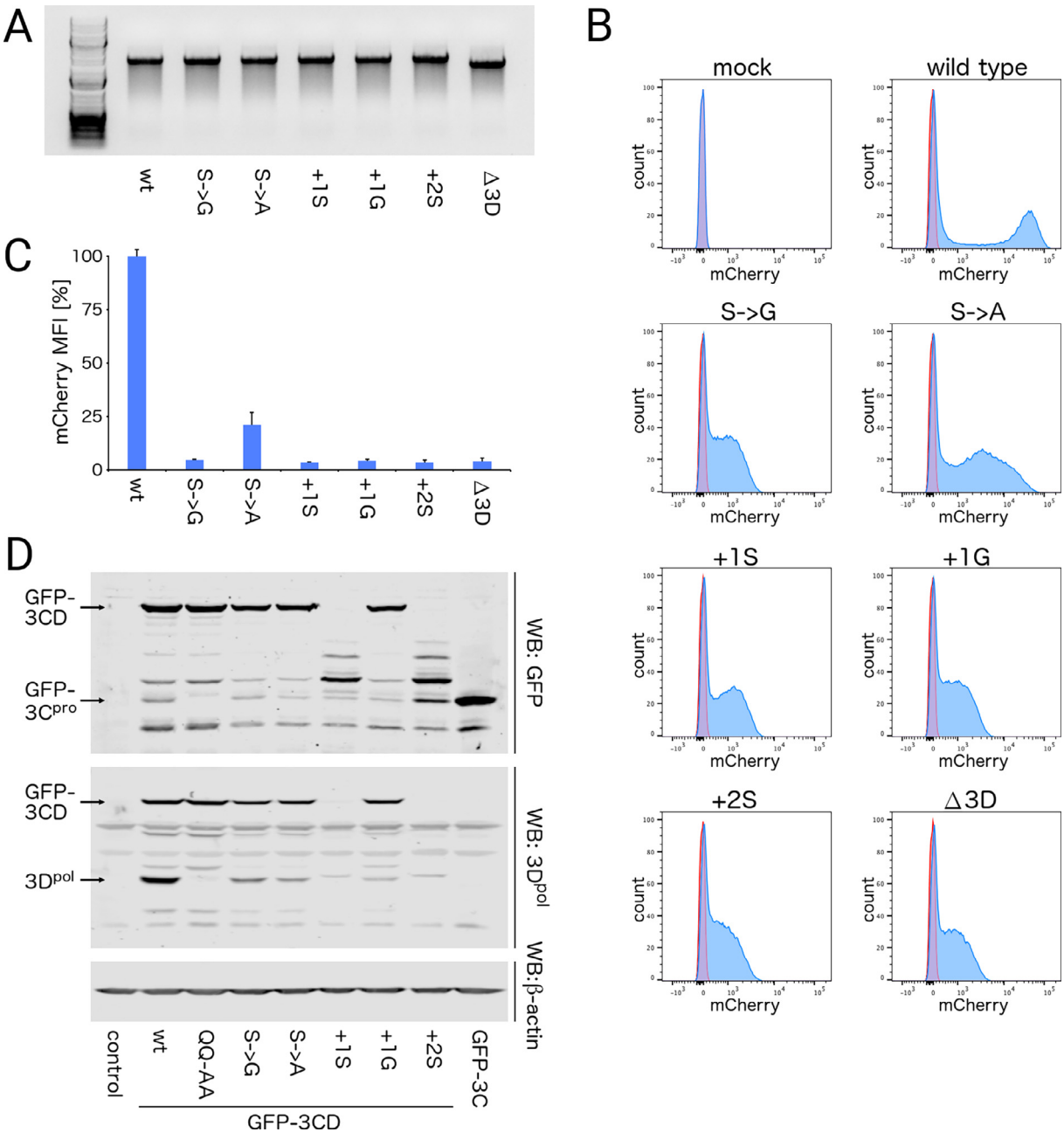

Fig. 3. FACS analysis of Aichi virus replication. A) Quality of RNA used for the viral replicon assay analyzed on the 1% agarose gel. B and C) Viral replicon assay. HeLa cells were transfected with the T7-amplified aichivirus subgenomic replicon wild-type RNA or its mutants within the $3D^{pol}$ region as indicated, and the reporter mCherry fluorescence was determined by flow cytometry. The data are presented as histograms of mCherry fluorescence from one representative experiment (B) or as the mean mCherry fluorescence ± standard error of the mean (SEM) from two independent experiments (C). D) AiV 3CD processing analysis. HEK293T cells were transfected with the EGFP-fused wild-type 3CD or its mutants as indicated, and the cell lysates were analyzed by immunoblotting using the anti-GFP and anti-AiV $3D^{pol}$ antibodies.

sicinivirus genera where most other members of the *Picornaviridae* family have a conserved glycine residue. Also all previously reported structures of picornaviral polymerases have the glycine residue in the first position. The $3D^{pol}$ N-terminus is liberated upon the cleavage of the stable 3CD precursor and is essential for the activation of the $3D^{pol}$ enzyme. At least two mechanisms how the $3D^{pol}$ N-terminus activates the polymerase activity were suggested. Campagnola et al. noticed a conserved hydrophobic residue (phenylalanine or tryptophan) at position 5 that is solvent exposed due to the unusual hydrogen bonding within the first two antiparallel β-sheets (Campagnola et al., 2008). This hydrophobic residue (Phe5 or Trp5) has a profound effect on the enzymatic activity because it is involved in the rate limiting NTP repositioning step through its interaction with the residue Tyr62. FMDV has an aspartate on the fifth position but this aspartate interacts with His64 which is structurally equivalent to Tyr62 (Ferrer-Orta et al., 2004). However, SiV $3D^{pol}$ has a glutamate residue and AiV $3D^{pol}$ a proline residue at position 5 (Fig. 1B). It is very unlikely that glutamate or proline and histidine could form a salt bridge in a similar fashion as aspartate and histidine as in the case of FMDV.

Based on the structure of the PV $3D^{pol}$ enzyme (Thompson and Peersen, 2004) it was also suggested that the function of the very first $3D^{pol}$ residue is to stabilize Asp238, a conserved residue located in a short α10 helix that forms a hydrogen bond with the 2′ hydroxyl group of incoming NTP nucleotide. This interaction is structurally conserved

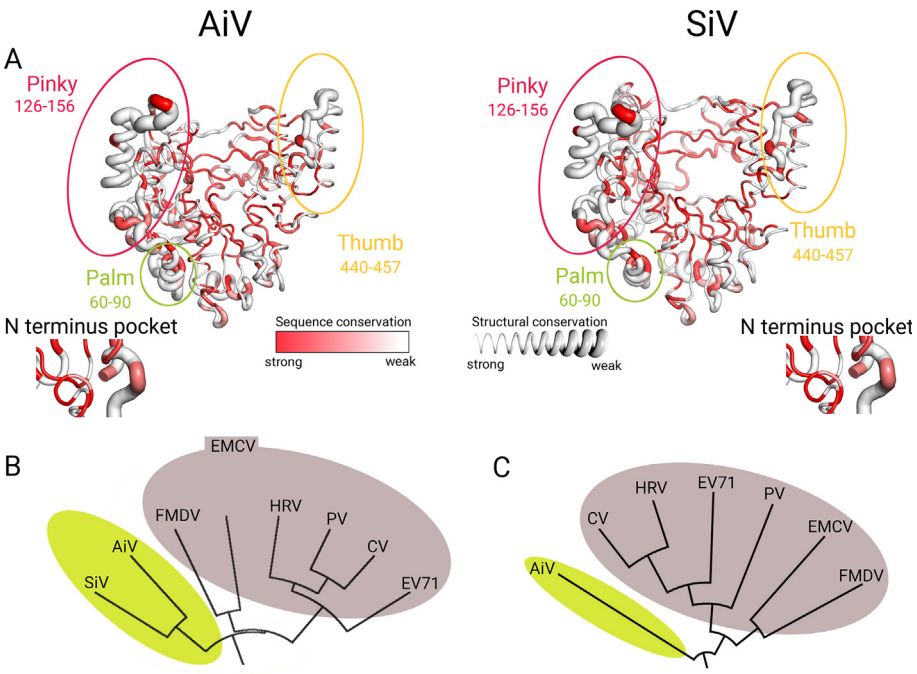

Fig. 4. Structural comparison of Aichi 3D^{pol} with other picornaviral 3D^{pol} enzymes. A) Sausage representation that illustrates the three-dimensional structure conservation of AiV and SiV 3D^{pol} according to thickness of the ribbon (the thickest is least conserved) and the conservation of primary sequence (least conserved regions are labeled in white). The radius of ribbons is proportional to the difference of Cα position between AiV or SiV 3D^{pol} and all homologous picornaviral polymerases of known structures. The major distinction was observed in the pinky and finger region and in helix α2. Structures of AiV and SiV polymerase are similar to each other's, but different to the others so far known 3D^{pol} structures of the *Picornaviridae* family. B) A structure based phylogenetic tree illustrating the apparent independent evolution of AiV and SiV polymerases. C) Analogous phylogenetic tree based on a structural alignment of capsid protomers from various picornaviruses is in agreement with the phylogenetic tree based on known 3D^{pol} structures.

in kobuviruses and sicinivirus. The first serine residue in AiV 3D^{pol} forms hydrogen bonds with His60, Gly63 and Ala240 to stabilize the α10 helix. The first serine residue of SiV forms a hydrogen bond and a water bridge with Ser239, a neighboring residue of Asp238 and thus also stabilizes the short α10 helix albeit using a different mechanism (Fig. 2). We conclude that activation of the α10 helix by the liberated N-terminus is a feature shared in all the structures of picornaviral polymerases and we suggest that this is the mechanism of 3D^{pol} activation upon proteolytical cleavage.

The N-termini of AiV and SiV 3D^{pol} are the least conserved regions when compared to other picornaviruses. We performed a structural comparison of the AiV and SiV 3D^{pol} enzymes with all the solved structures of picornaviral 3D^{pol} enzymes available in the PDB database using the ENDscript 2.0 (Robert and Gouet, 2014) (Fig. 4, low conserved regions are in thick ribbons). The analysis revealed that besides the N-termini also the helix α2, and the pinky and thumb fingers of the AiV and SiV 3D^{pol} are low conserved regions.

Next, we constructed a phylogenetic tree based on all the solved 3D^{pol} structures available in the PDB database by the lowest RMSD (root-mean-square deviation of atomic positions) method which illustrates that kobuviruses and sicinivirus are evolutionary distinct group within the *Picornaviridae* family (Fig. 4B). Very similar results were obtained when structures of viral capsid proteins were used (Fig. 4C) (Sabin et al., 2016) suggesting that the polymerase and the viral capsid started to evolve separately from other picornaviruses at the same time. This analysis sets the kobuvirus and sicinivirus genera apart from other picornaviruses, however, it also highlights the conserved mechanism of 3D^{pol} activation upon proteolytical processing.

4. Materials and methods

Protein expression and purification – Artificial codon optimized genes encoding the AiV and SiV 3D^{pol} enzymes (UniProtKB – B8R1T8_9PICO, A0A0P0QLC4_9PICO) were commercially synthesized (Invitrogen) and cloned into a pSUMO vector resulting into genes encoding for His_{8x}SUMO-3D^{pol} fusion proteins. To improve crystallization properties we introduced surface entropy reduction mutations (K57A, Q58A, R118L for SiV 3D^{pol} and E93,94A for AiV 3D^{pol}) (Goldschmidt et al., 2007). The protein was expressed and purified using our standard protocols for viral polymerases (Dubankova and Boura, 2019; Sebera et al., 2018). Briefly, it was expressed in the *E. coli* strain BL21 Star. After lysis the protein was immobilized on the NiNTA Agarose resin (Machery-Nagel) and extensively washed with the wash buffer (50 mM Tris pH = 8, 300 mM NaCl, 20 mM imidazole, 3 mM βME) and eluted with the wash buffer supplemented by 300 mM imidazole. The His_{8x}SUMO tag was cleaved by the Ulp1 protease and the protein was further purified by size exclusion chromatography. Finally, the protein was concentrated to 6 mg/ml and stored at −80 °C until needed.

Rabbit polyclonal antiserum against AiV 3D^{pol} was generated commercially (Exbio) using the recombinant AiV 3D^{pol} protein as immunogen. The polyclonal antibody to AiV 3D^{pol} was further purified by affinity chromatography using the HiTrap Protein A HP column (GE Healthcare) and then using the immunogen (AiV 3D^{pol})-coupled agarose beads AminoLink Coupling Resin (Thermo Fisher Scientific) according to the manufacturer's instructions.

Tissue cultures and transfections – Human HeLa and HEK293T were maintained in Dulbecco's modified Eagle's medium (Sigma) supplemented with 10% fetal calf serum (Gibco). RNA transfections of HeLa cells were carried out using the TransIT mRNA transfection kit (Mirus Bio). DNA transfections of HEK293T cells were performed using polyethylenimine (Sigma).

Viral subgenomic replicon assay – For viral subgenomic replicon assays, the pUCSF-AiV/mCherry plasmid was generated by replacing the capsid region within the pUCSF-AiV plasmid (kind gift of Prof. Joseph DeRisi, UCSF School of Medicine, San Francisco, USA) with the mCherry-encoding gene by restriction-free cloning. Further mutations within the 3D^{pol} encoding region were generated using the Q5 Site-Directed Mutagenesis Kit (New England BioLabs). All DNA constructs were verified by sequencing.

The pUCSF-AiV/mCherry wild-type and mutant plasmids were linearized by cleavage with HindIII-HF (Thermo Fisher Scientific) and purified using the mini spin columns (Epoch Life Science). Viral subgenomic replicon RNA was generated with TranscriptAid T7 High Yield Transcription Kit (Thermo Fisher Scientific) and purified using the RNeasy mini spin columns (Qiagen). For replicon assays, HeLa cells grown in 12-well plates were transfected with T7-amplified RNA using the TransIT mRNA transfection kit (Mirus Bio). At 9 h post transfection, the reporter mCherry fluorescence was determined by flow cytometry using BD LSR Fortessa (BD Biosciences) and the following optical configuration: 561 nm laser, 670/30 nm bandpass filter. Acquired data

were analyzed with the FlowJo software.

Western blotting and immunodetection – HEK293T cells grown in 6-well plates were transfected with the appropriate mutants of the EGFP-fused AiV 3CD protein using polyethylenimine (Sigma). Next day, the cells were harvested, washed twice with phosphate-buffered saline and lysed in the ice-cold lysis buffer (20 mM Tris pH 7.4, 100 mM NaCl, 50 mM NaF, 10 mM EDTA, 10% glycerol, 1% NP-40), supplemented with protease inhibitors (Complete protease inhibitor cocktail, Sigma). After solubilizing for 15 min on ice, the lysates were pre-cleared by centrifugation at 16,000g for 15 min. The resulting supernatants were mixed with the Laemmli sample buffer, boiled for 5 min, subjected to SDS-PAGE using the 15% polyacrylamide gels, Western-blotted onto nitrocellulose membranes (Thermo Fisher Scientific), and stained with the following antibodies: rabbit polyclonal antibody to GFP (Cell Signaling #2956), rabbit polyclonal antibody to AiV $3D^{pol}$ (home-made), and mouse monoclonal antibody to β-actin (Sigma #A5441). The images were acquired using the LI-COR Odyssey Infrared Imaging System.

Crystallization – Crystals grew in sitting drops in 1–2 days at 18 °C. Drops were set up from 50% of protein solution and 50% of precipitant. 12,5% PEG 1000, 12,5% PEG 3350, 12,5% (RS)-2-methyl-2,4-pentanediol, 0,2 M 0.2 M 1,6-hexanediol, 0.2 M 1-butanol, 0.2 M (RS)-1,2-propanediol, 0.2 M 2-propanol, 0.2 M 1,4-butanediol, 0.2 M 1,3-propanediol and 0,1 M MES/Imidazole pH 6.5 was used for the SiV $3D^{pol}$ and 1.7 M $(NH_4)_2SO_4$, 1.7% (v/v) PEG400, 15% (v/v) glycerol, 85 mM HEPES pH 7.5 for the AiV $3D^{pol}$.

Crystals were flash frozen in liquid nitrogen and diffraction data were collected at the 14.1 BESSY beamline in HZB synchrotron facility (Mueller et al., 2012).

Data analysis – Diffraction data were processed using XDS (Kabsch, 2010), Phenix (Adams et al., 2010) and CCP4 (Winn et al., 2011) packages. Molecular replacement was done with a polyalanine model based on the structure of EMCV $3D^{pol}$ (PDB ID: 4nz0) (Vives-Adrian et al., 2014). Structural figures were generated by PyMol (Schrodinger). The electrostatic surface was calculated using plugin APBS Tools (Baker et al., 2001). The structural alignment was done in Multiseq tool in VMD, STAMP (Roberts et al., 2006) and the phylogenetic tree was visualized in FigTree interaface (http://tree.bio.ed.ac.uk/software/figtree/).

5. Accession numbers

The crystal structures of the SiV and AiV $3D^{pol}$ enzyme were deposited in the PDB database under codes 6QWT and 6R1I.

Author contributions

AD, VH, and MK performed all experiments, analyzed data and prepared figures. EB designed the study, supervised the project and wrote the manuscript.

Declaration of Competing Interest

The authors declare that they have no known competing financial interests or personal relationships that could have appeared to influence the work reported in this paper.

Acknowledgements

We are grateful to Prof. Joseph DeRisi (UCSF School of Medicine, San Francisco, USA) for providing the pUCSF-AiV plasmid encoding the synthetically constructed complete aichivirus genome. We thank HZB for the allocation of synchrotron radiation beamtime. The work was supported from European Regional Development Fund; OP RDE; Project: “Chemical biology for drugging undruggable targets (ChemBioDrug)” (No. CZ.02.1.01/0.0/0.0/16_019/0000729) and by the Czech Science Foundation (grant number 17-07058Y). The Academy of Sciences of Czech Republic support (RVO:61388963) is also acknowledged.

Appendix A. Supplementary data

Supplementary data to this article can be found online at https://doi.org/10.1016/j.jsb.2019.08.004.

References

Adams, P.D., Afonine, P.V., Bunkoczi, G., Chen, V.B., Davis, I.W., Echols, N., Headd, J.J., Hung, L.W., Kapral, G.J., Grosse-Kunstleve, R.W., McCoy, A.J., Moriarty, N.W., Oeffner, R., Read, R.J., Richardson, D.C., Richardson, J.S., Terwilliger, T.C., Zwart, P.H., 2010. PHENIX: a comprehensive Python-based system for macromolecular structure solution. Acta Crystallogr. Sect. D, Biol. Crystallogr. 66, 213–221.

Altan-Bonnet, N., 2017. Lipid tales of viral replication and transmission. Trends Cell Biol. 27, 201–213.

Andino, R., Domingo, E., 2015. Viral quasispecies. Virology 479–480, 46–51.

Baker, N.A., Sept, D., Joseph, S., Holst, M.J., McCammon, J.A., 2001. Electrostatics of nanosystems: application to microtubules and the ribosome. Proc. Natl. Acad. Sci. U.S.A. 98, 10037–10041.

Bullman, S., Kearney, K., O'Mahony, M., Kelly, L., Whyte, P., Fanning, S., Morgan, J.G., 2014. Identification and genetic characterization of a novel picornavirus from chickens. J. Gen. Virol. 95, 1094–1103.

Campagnola, G., Weygandt, M., Scoggin, K., Peersen, O., 2008. Crystal structure of coxsackievirus B3 3Dpol highlights the functional importance of residue 5 in picornavirus polymerases. J. Virol. 82, 9458–9464.

Dubankova, A., Boura, E., 2019. Structure of the yellow fever NS5 protein reveals conserved drug targets shared among flaviviruses. Antiviral Res. 169, 104536.

Dubankova, A., Humpolickova, J., Klima, M., Boura, E., 2017. Negative charge and membrane-tethered viral 3B cooperate to recruit viral RNA dependent RNA polymerase 3D (pol). Sci. Rep. 7, 17309.

Ferrer-Orta, C., Arias, A., Escarmis, C., Verdaguer, N., 2006. A comparison of viral RNA-dependent RNA polymerases. Curr. Opin. Struct. Biol. 16, 27–34.

Ferrer-Orta, C., Arias, A., Perez-Luque, R., Escarmis, C., Domingo, E., Verdaguer, N., 2004. Structure of foot-and-mouth disease virus RNA-dependent RNA polymerase and its complex with a template-primer RNA. J. Biol. Chem. 279, 47212–47221.

Ferrer-Orta, C., Arias, A., Perez-Luque, R., Escarmis, C., Domingo, E., Verdaguer, N., 2007. Sequential structures provide insights into the fidelity of RNA replication. Proc. Natl. Acad. Sci. U.S.A. 104, 9463–9468.

Gohara, D.W., Ha, C.S., Kumar, S., Ghosh, B., Arnold, J.J., Wisniewski, T.J., Cameron, C.E., 1999. Production of “authentic” poliovirus RNA-dependent RNA polymerase (3D(pol)) by ubiquitin-protease-mediated cleavage in Escherichia coli. Protein Expr. Purif. 17, 128–138.

Goldschmidt, L., Cooper, D.R., Derewenda, Z.S., Eisenberg, D., 2007. Toward rational protein crystallization: a Web server for the design of crystallizable protein variants. Protein Sci.: A Publ. Protein Soc. 16, 1569–1576.

Gong, P., Peersen, O.B., 2010. Structural basis for active site closure by the poliovirus RNA-dependent RNA polymerase. Proc. Natl. Acad. Sci. U.S.A. 107, 22505–22510.

Gong, P., Kortus, M.G., Nix, J.C., Davis, R.E., Peersen, O.B., 2013. Structures of coxsackievirus, rhinovirus, and poliovirus polymerase elongation complexes solved by engineering RNA mediated crystal contacts. PLoS ONE 8, e60272.

Greninger, A.L., Knudsen, G.M., Betegon, M., Burlingame, A.L., Derisi, J.L., 2012. The 3A protein from multiple picornaviruses utilizes the golgi adaptor protein ACBD3 to recruit PI4KIIIbeta. J. Virol. 86, 3605–3616.

Hansen, J.L., Long, A.M., Schultz, S.C., 1997. Structure of the RNA-dependent RNA polymerase of poliovirus. Structure 5, 1109–1122.

Harak, C., Lohmann, V., 2015. Ultrastructure of the replication sites of positive-strand RNA viruses. Virology 479, 418–433.

Harris, K.S., Reddigari, S.R., Nicklin, M.J., Hammerle, T., Wimmer, E., 1992. Purification and characterization of poliovirus polypeptide 3CD, a proteinase and a precursor for RNA polymerase. J. Virol. 66, 7481–7489.

Horova, V., Lyoo, H., Rozycki, B., Chalupska, D., Smola, M., Humpolickova, J., Strating, J., van Kuppeveld, F.J.M., Boura, E., Klima, M., 2019. Convergent evolution in the mechanisms of ACBD3 recruitment to picornavirus replication sites. PLoS Pathog. 15, e1007962.

Hsu, N.Y., Ilnytska, O., Belov, G., Santiana, M., Chen, Y.H., Takvorian, P.M., Pau, C., van der Schaar, H., Kaushik-Basu, N., Balla, T., Cameron, C.E., Ehrenfeld, E., van Kuppeveld, F.J., Altan-Bonnet, N., 2010. Viral reorganization of the secretory pathway generates distinct organelles for RNA replication. Cell 141, 799–811.

Kabsch, W., 2010. Xds. Acta Crystallogr. Sect. D, Biol. Crystallogr. 66, 125–132.

Kitajima, M., Gerba, C.P., 2015. Aichi virus 1: environmental occurrence and behavior. Pathogens 4, 256–268.

Klima, M., Chalupska, D., Rozycki, B., Humpolickova, J., Rezabkova, L., Silhan, J., Baumlova, A., Dubankova, A., Boura, E., 2017. Kobuviral non-structural 3A proteins act as molecular harnesses to hijack the host ACBD3 protein. Structure 25, 219–230.

Klima, M., Toth, D.J., Hexnerova, R., Baumlova, A., Chalupska, D., Tykvart, J., Rezabkova, L., Sengupta, N., Man, P., Dubankova, A., Humpolickova, J., Nencka, R., Veverka, V., Balla, T., Boura, E., 2016. Structural insights and in vitro reconstitution of membrane targeting and activation of human PI4KB by the ACBD3 protein. Sci. Rep. 6, 23641.

Love, R.A., Maegley, K.A., Yu, X., Ferre, R.A., Lingardo, L.K., Diehl, W., Parge, H.E., Dragovich, P.S., Fuhrman, S.A., 2004. The crystal structure of the RNA-dependent RNA polymerase from human rhinovirus: a dual function target for common cold antiviral therapy. Structure 12, 1533–1544.

Marcotte, L.L., Wass, A.B., Gohara, D.W., Pathak, H.B., Arnold, J.J., Filman, D.J., Cameron, C.E., Hogle, J.M., 2007. Crystal structure of poliovirus 3CD protein: virally encoded protease and precursor to the RNA-dependent RNA polymerase. J. Virol. 81, 3583–3596.

McPhail, J.A., Ottosen, E.H., Jenkins, M.L., Burke, J.E., 2017. The molecular basis of Aichi virus 3A protein activation of phosphatidylinositol 4 kinase IIIbeta, PI4KB, through ACBD3. Structure 25, 121–131.

Mejdrova, I., Chalupska, D., Kogler, M., Sala, M., Plackova, P., Baumlova, A., Hrebabecky, H., Prochazkova, E., Dejmek, M., Guillon, R., Strunin, D., Weber, J., Lee, G., Birkus, G., Mertlikova-Kaiserova, H., Boura, E., Nencka, R., 2015. Highly selective phosphatidylinositol 4-kinase IIIbeta inhibitors and structural insight into their mode of action. J. Med. Chem. 58, 3767–3793.

Mejdrova, I., Chalupska, D., Plackova, P., Muller, C., Sala, M., Klima, M., Baumlova, A., Hrebabecky, H., Prochazkova, E., Dejmek, M., Strunin, D., Weber, J., Lee, G., Matousova, M., Mertlikova-Kaiserova, H., Ziebuhr, J., Birkus, G., Boura, E., Nencka, R., 2017. Rational design of novel highly potent and selective phosphatidylinositol 4-kinase IIIbeta (PI4KB) inhibitors as broad-spectrum antiviral agents and tools for chemical biology. J. Med. Chem. 60, 100–118.

Mueller, U., Darowski, N., Fuchs, M.R., Forster, R., Hellmig, M., Paithankar, K.S., Puhringer, S., Steffien, M., Zocher, G., Weiss, M.S., 2012. Facilities for macromolecular crystallography at the Helmholtz-Zentrum Berlin. J. Synchrotron Radiat. 19, 442–449.

Nagy, P.D., Strating, J.R., van Kuppeveld, F.J., 2016. Building viral replication organelles: close encounters of the membrane types. PLoS Pathog. 12, e1005912.

Paul, A.V., van Boom, J.H., Filippov, D., Wimmer, E., 1998. Protein-primed RNA synthesis by purified poliovirus RNA polymerase. Nature 393, 280–284.

Peersen, O.B., 2017. Picornaviral polymerase structure, function, and fidelity modulation. Virus Res.

Robert, X., Gouet, P., 2014. Deciphering key features in protein structures with the new ENDscript server. Nucleic Acids Res. 42, W320–W324.

Roberts, E., Eargle, J., Wright, D., Luthey-Schulten, Z., 2006. MultiSeq: unifying sequence and structure data for evolutionary analysis. BMC Bioinf. 7, 382.

Sabin, C., Fuzik, T., Skubnik, K., Palkova, L., Lindberg, A.M., Plevka, P., 2016. Structure of Aichi virus 1 and its empty particle: clues towards kobuvirus genome release mechanism. J. Virol.

Sasaki, J., Ishikawa, K., Arita, M., Taniguchi, K., 2012. ACBD3-mediated recruitment of PI4KB to picornavirus RNA replication sites. EMBO J. 31, 754–766.

Sebera, J., Dubankova, A., Sychrovsky, V., Ruzek, D., Boura, E., Nencka, R., 2018. The structural model of Zika virus RNA-dependent RNA polymerase in complex with RNA for rational design of novel nucleotide inhibitors. Sci. Rep. 8, 11132.

Sun, D., Chen, S., Cheng, A., Wang, M., 2016. Roles of the picornaviral 3C proteinase in the viral life cycle and host cells. Viruses 8, 82.

Thompson, A.A., Peersen, O.B., 2004. Structural basis for proteolysis-dependent activation of the poliovirus RNA-dependent RNA polymerase. EMBO J. 23, 3462–3471.

Vives-Adrian, L., Lujan, C., Oliva, B., van der Linden, L., Selisko, B., Coutard, B., Canard, B., van Kuppeveld, F.J., Ferrer-Orta, C., Verdaguer, N., 2014. The crystal structure of a cardiovirus RNA-dependent RNA polymerase reveals an unusual conformation of the polymerase active site. J. Virol. 88, 5595–5607.

Winn, M.D., Ballard, C.C., Cowtan, K.D., Dodson, E.J., Emsley, P., Evans, P.R., Keegan, R.M., Krissinel, E.B., Leslie, A.G., McCoy, A., McNicholas, S.J., Murshudov, G.N., Pannu, N.S., Potterton, E.A., Powell, H.R., Read, R.J., Vagin, A., Wilson, K.S., 2011. Overview of the CCP4 suite and current developments. Acta Crystallogr. Sect. D, Biol. Crystallogr. 67, 235–242.

Wu, Y., Lou, Z., Miao, Y., Yu, Y., Dong, H., Peng, W., Bartlam, M., Li, X., Rao, Z., 2010. Structures of EV71 RNA-dependent RNA polymerase in complex with substrate and analogue provide a drug target against the hand-foot-and-mouth disease pandemic in China. Protein Cell 1, 491–500.

Yamashita, T., Kobayashi, S., Sakae, K., Nakata, S., Chiba, S., Ishihara, Y., Isomura, S., 1991. Isolation of cytopathic small round viruses with BS-C-1 cells from patients with gastroenteritis. J. Infect. Dis. 164, 954–957.